Supplemental Material can be found at:
http://www.jbc.org/content/suppl/2012/01/24/M111.294272.DC1.html

THE JOURNAL OF BIOLOGICAL CHEMISTRY VOL. 287, NO. 11, pp. 8621–8632, March 9, 2012
© 2012 by The American Society for Biochemistry and Molecular Biology, Inc. Published in the U.S.A.

# Critical Role of N-terminal End-localized Nuclear Export Signal in Regulation of Activating Transcription Factor 2 (ATF2) Subcellular Localization and Transcriptional Activity*[S]

Received for publication, August 18, 2011, and in revised form, January 23, 2012 Published, JBC Papers in Press, January 24, 2012, DOI 10.1074/jbc.M111.294272

**Chih-Chao Hsu**[1] **and Chang-Deng Hu**[2]

*From the Department of Medicinal Chemistry and Molecular Pharmacology and the Purdue University Center for Cancer Research, Purdue University, West Lafayette, Indiana 47907*

**Background:** Alteration of ATF2 subcellular localization is involved in multiple human diseases.
**Results:** A second nuclear export signal was identified in the most N-terminal end of ATF2.
**Conclusion:** The newly identified nuclear export signal negatively regulates ATF2 nuclear localization and transcriptional activity.
**Significance:** Understanding how ATF2 subcellular localization is regulated will provide insight into the pathological role of ATF2 in human diseases.

**Activating transcription factor 2 (ATF2) belongs to the basic leucine zipper family of transcription factors. ATF2 regulates target gene expression by binding to the cyclic AMP-response element as a homodimer or a heterodimer with c-Jun. Cytoplasmic localization of ATF2 was observed in melanoma, brain tissue from patients with Alzheimer disease, prostate cancer specimens, and ionizing radiation-treated prostate cancer cells, suggesting that alteration of ATF2 subcellular localization may be involved in the pathogenesis of these diseases. We previously demonstrated that ATF2 is a nucleocytoplasmic shuttling protein, and it contains two nuclear localization signals in the basic region and one nuclear export signal (NES) in the leucine zipper domain (named LZ-NES). In the present study, we demonstrate that a hydrophobic stretch in the N terminus, $^{1}$MKFKLHV$^{7}$, also functions as an NES (termed N-NES) in a chromosome region maintenance 1 (CRM1)-dependent manner. Mutation of both N-NES and LZ-NES results in a predominant nuclear localization, whereas mutation of each individual NES only partially increases the nuclear localization. These results suggest that cytoplasmic localization of ATF2 requires function of at least one of the NESs. Further, mutation of N-NES enhances the transcriptional activity of ATF2, suggesting that the novel NES negatively regulates the transcriptional potential of ATF2. Thus, ATF2 subcellular localization is probably modulated by multiple mechanisms, and further understanding of the regulation of ATF2 subcellular localization under various pathological conditions will provide insight into the pathophysiological role of ATF2 in human diseases.**

ATF2 (activating transcription factor 2) is a basic leucine zipper (bZIP)[3] protein and is an important member of the activator protein-1 (AP-1) family (1). Like other bZIP transcription factors, ATF2 utilizes its basic region to bind DNA and its leucine zipper region to dimerize with its partners. ATF2 binds the cAMP-response element, T(G/T)ACGTCA, as a homodimer or ATF2·c-Jun heterodimer (2–4), and regulates transcription of a large set of genes, including those involved in anti-apoptosis (5, 6), cell growth (7, 8), and DNA damage response (9).

The transcriptional activity of ATF2 can be regulated by multiple mechanisms. First, the transcriptional activity of ATF2 is regulated by phosphorylation at Thr-69 and Thr-71 within the N-terminal transactivation domain (10–12). In response to growth and stress signals, these two residues can be phosphorylated by mitogen-activated protein kinases (MAPKs), including extracellular signal regulated kinase (ERK), c-Jun N-terminal kinase (JNK), and p38 (10–12). The phosphorylation-induced transcriptional activity may be achieved by increasing the intrinsic histone acetylase activity of ATF2 (13), promoting DNA binding (14), and/or preventing it from ubiquitination (15, 16). Second, the transcriptional activity of ATF2 is regulated by an intramolecular interaction between the N-terminal transactivation domain and the bZIP domain (17). This is largely based on the observation that the activity of ATF2 is limited when it is exogenously expressed without coexpression with its dimerization partners or coactivators (17–20). It was proposed that the activity of ATF2 is repressed by an intramolecular interaction between the N-terminal domain and the bZIP domain (17). However, when coexpressed with coactivators, such as CREB-binding protein or E1A (21), the intramolecular interaction is disrupted. Third, the transcriptional activity is regulated by its subcellular localization. We recently demonstrated that ATF2 is a nucleocytoplasmic shuttling protein, and its subcellular localization is regulated by its

* This work is supported in part by grants from the National Science Foundation, American Heart Association, and the United States Department of Defense and by Purdue University Center for Cancer Research Small Grants.
[S] This article contains supplemental Figs. 1–9.
[1] Supported by the Purdue Research Foundation Graduate Fellowship and Ronal W. Dollens Graduate Scholarship in the Life Sciences.
[2] To whom correspondence should be addressed: 575 Stadium Mall Dr., West Lafayette, Indiana 47907. Tel.: 765-496-1971; Fax: 765-494-1414; E-mail: hu1@purdue.edu.

[3] The abbreviations used are: bZIP, basic leucine zipper; NLS, nuclear localization signal; NES, nuclear export signal; LMB, leptomycin B; CREB, cAMP-response element-binding protein; IP, immunoprecipitation; NTD, N-terminal domain.

Downloaded from www.jbc.org at Purdue University Libraries, on September 24, 2012

dimerization (19). Interestingly, overexpressed ATF2 is predominantly localized in the cytoplasm due to the inadequate level of Jun proteins anchoring ATF2 in the nucleus (19). This finding not only uncovers a novel regulatory mechanism of ATF2 transcriptional activity but also provides an alternative mechanism, that the limited transcriptional activity of overexpressed ATF2 may be due to its insufficient nuclear localization in addition to the intramolecular interaction.

Alteration of ATF2 subcellular localization appears to be implicated in the pathogenesis of several human diseases. In melanoma specimens, cytoplasmic localized ATF2 is associated with a better outcome, whereas strong nuclear staining correlates with a poor prognosis (22). In skin cancer, reduced nuclear ATF2 was observed in most basal and squamous cell carcinoma cells (23). In the brain, cytoplasmic ATF2 was observed in cortical neurons of patients with Alzheimer disease (24). In prostate cancer, increased cytoplasmic phosphorylated ATF2 was linked to disease progression (25). Moreover, we recently reported that ionizing radiation-induced cytoplasmic sequestration of ATF2 is involved in neuroendocrine differentiation in prostate cancer cells (26, 27). Although the impact of ATF2 subcellular localization appears to be dependent on disease context, these reports highlight the importance of understanding the molecular mechanisms regulating ATF2 subcellular localization.

Currently, the mechanism by which ATF2 subcellular localization is regulated is not well understood. We have found that ATF2 is a nucleocytoplasmic shuttling protein with a nuclear export signal (NES) and two nuclear localization signals (NLSs) in its leucine zipper and basic region, respectively (19). We have also demonstrated that heterodimerization with the Jun family proteins anchors ATF2 in the nucleus by preventing its nuclear export. On the contrary, homodimerization of ATF2 in the cytoplasm hampers the nuclear import (19). Here, we further show that ATF2 possesses another NES located in the most N-terminal end, which functions in cooperation with the previously identified NES to export ATF2 out of the nucleus. Importantly, this NES negatively regulates ATF2 transcriptional activity.

## EXPERIMENTAL PROCEDURES

*Antibodies*—Monoclonal anti-FLAG M2 antibody and monoclonal anti-hemagglutinin (HA) antibody were purchased from Sigma. Monoclonal anti-Myc antibody is from Clontech (Palo Alto, CA). Monoclonal anti-phospho-ATF2 (Thr(P)-71) antibody (sc-8398), polyclonal anti-GFP antibody (sc-8334), and anti-c-Jun antibody (sc-1694) were obtained from Santa Cruz Biotechnology, Inc. (Santa Cruz, CA).

*Plasmid Construction*—Localization of wild-type and mutant ATF2 proteins was determined by expressing ATF2 as fusion proteins with Venus(A206K), a monomeric mutant of Venus (28–30). A flexible poly-glycine-serine linker $(GGGGS)_3$ was introduced to the N terminus of Venus (A206K) by PCR. The amplified cDNA encoding $(GGGGS)_3$-Venus(A206K) was cloned into the SalI/BamHI site of pFLAG-CMV2 (Sigma) to produce pFLAG-$(4G1S)_3$-Venus(A206K). cDNAs encoding wild-type and all mutant ATF2 proteins were cloned in frame into NotI/KpnI sites of pFLAG-$(4G1S)_3$-Venus(A206K). All deletions and mutations of ATF2 were made by PCR or ligation PCR (31), and cDNAs encoding these mutant ATF2 proteins were subcloned into pFLAG-$(4G1S)_3$-Venus(A206K). For luciferase reporter gene assays, cDNAs encoding ATF2(N-NES4A), ATF2(LZ-NES3A), and ATF2(N/LZ-NESm) were released from the Venus(A206K) fusion constructs and were subcloned into NotI/KpnI sites of pFLAG-CMV2. To generate C-terminal Myc tag fusion protein, sequence encoding Myc epitope (MASMQKLISEEDL) was introduced in frame downstream of the BamHI site by the PCR method to produce pFLAG-MCS-Myc. The cDNA encoding wild-type or mutant ATF2 was then subcloned into NotI/KpnI sites of pFLAG-MCS-Myc. To make double Venus(A206K) fusion proteins, a PCR-amplified DNA fragment encoding Venus(A206K) was cloned into KpnI/SalI sites of pFLAG-$(4G1S)_3$-Venus(A206K) to produce pFLAG-2xVenus(A206K). PCR-amplified DNA fragments encoding ATF2(1–73) and ATF2(1–73, N-NES4A) were then cloned into NotI/KpnI sites of pFLAG-2xVenus-(A206K) to generate pFLAG-ATF2(1–73)-2xVenus(A206K) and pFLAG-ATF2(1–73, N-NES4A)-2xVenus(A206K), respectively. All constructs generated by the PCR-based method were confirmed by DNA sequencing. The *jun2-luc* reporter plasmid was a gift from Dr. Dorien Peters (32). LZ-NES3A is a substitution of three leucine residues in the NES in the leucine zipper region. N-NES4A, PNES1m, PNES2m, PNES3m, and PNES4m are substitutions of hydrophobic residues in the putative NES within the ATF2 N-terminal domain (NTD), as shown in Figs. 2*A* and 4*B*.

*Cell Culture and Fluorescence Imaging Analysis*—COS-1 cells were cultured in Dulbecco's modified Eagle's medium supplemented with 5% fetal bovine serum and antibiotics at 37 °C in 5% $CO_2$. Forty thousand cells per well were seeded in 12-well plates to grow overnight and then transfected with 2 $\mu$g of expression vectors indicated in each experiment using Fugene 6 (Roche Applied Science). At 16–18 h post-transfection, cells were fixed with 3.7% formaldehyde in phosphate-buffered saline (PBS) for 20 min. To inhibit nuclear export of ATF2 fusion proteins, transfected cells, at 14 h after transfection, were treated with 20 ng/ml leptomycin B (LMB) for 3.5 h before fixation. Fixed cells were permeabilized with 0.2% Triton X-100 in PBS for 5 min followed by counterstaining with 2.5 $\mu$g/ml 4′,6-diamidino-2-phenylindole (DAPI) to visualize nuclei. Localization of various ATF2-Venus(A206K) fusion proteins were examined by a Nikon TE2000-U inverted fluorescence microscope with YFP filters as reported previously (19). All images for purposes of quantification were taken at ×300 magnification. To determine ATF2 localization, five regions of interest, with a diameter of ~4.5 $\mu$m, were randomly selected from the nucleus and perinuclear regions, respectively, followed by measuring the intensity of Venus fluorescence within regions of interest using MetaMorph II software. The acquired emission intensities were background-corrected by subtracting mean fluorescence intensity of fields without cells. The localization of wild-type or mutant ATF2-Venus(A206K) within a cell was determined by calculating the ratio of mean nuclear fluorescence intensity to mean cytoplasmic fluorescence intensity. More than 50 individual cells were quantified in each set of experiments, and the ratio of nuclear to cytoplasmic intensity of each fusion protein was presented as mean ± S.E. from at least

Downloaded from www.jbc.org at Purdue University Libraries, on September 24, 2012

three independent experiments. The integrity of all Venus fusion proteins was confirmed by Western blot (supplemental Fig. 1).

*Co-Immunoprecipitation (Co-IP)*—To determine the interaction between CRM1 (chromosome region maintenance 1) and N-NES, COS-1 cells cultured in a 10-cm dish were co-transfected with 5 μg of pMyc-CRM1 and 5 μg of pFLAG-Venus(A206K)-ATF2(1–341) or pFLAG-Venus(A206K)-ATF2(1–341, N-NES4A) for 2 days. Cells were trypsinized and resuspended in co-IP buffer (50 mM Tris-HCl, pH 7.4, 100 mM NaCl, 10 mM EDTA, 0.1% Triton X-100, 1 mM DTT, 5 μg/ml chymostatin, 5 μg/ml pepstatin A, 5 μg/ml leupeptin, 5 μg/ml antipain, and 5 mM PMSF). Cells were then sonicated to disrupt plasma and nuclear membrane, followed by centrifugation at 14,000 rpm for 10 min at 4 °C. The supernatant containing whole cell lysate (800 μg) was subjected to co-IP using 10 μg of anti-FLAG antibody for 2 h at 4 °C, followed by incubation with protein G beads (Santa Cruz Biotechnology, Inc.) for another 2 h at 4 °C. Bead-bound immune complexes were washed with co-IP buffer four times and subjected to SDS-PAGE followed by immunoblotting analysis with anti-Myc and anti-FLAG antibodies.

To determine the effect of the LZ-NES mutation on ATF2·c-Jun heterodimerization, HEK 293T cells were transfected with 5 μg of FLAG-ATF2-Venus(A206K) or FLAG-ATF2(LZ-NES3A)-Venus(A206K) for 1 day. Cell lysate was prepared as described above and then subjected to co-IP with anti-FLAG antibody (10 μg) at 4 °C overnight, followed by incubation with protein G beads at 4 °C for 2 h. The beads were washed with co-IP buffer six times with a 3-min rotation at 4 °C each time. The associated c-Jun was then detected by Western blot.

*Luciferase Reporter Gene Assay*—COS-1 cells were cultured in 12-well plates and serum-starved for 18 h. Cells were transfected with 2 μg of each indicated plasmid along with 0.5 μg of the *jun2-luc* reporter plasmid (luciferase reporter construct driven by five tandem repeats of *Jun2*) (32) and 100 ng of pRL-TK (Promega) for 24 h. Firefly and *Renilla* luciferase activities were measured by the Dual Luciferase Reporter Assay kit (Promega) according to the manufacturer's protocol with the following minor modifications. Firefly luciferase activity was measured by mixing 10 μl of cell lysate with 50 μl of LARII reagent. *Renilla* luciferase activity was then determined by mixing the sample with 50 μl of Stop & Glo reagent. The luciferase activity was measured by a TopCount NXT microplate luminescence counter (Packard). Luciferase data were presented as mean ± S.E. from at least three independent experiments performed in duplicate.

*Immunostaining*—COS-1 cells were fixed at 16 h post-transfection or at the end of LMB treatment with 3.7% formaldehyde for 20 min. Cells were then permeabilized with 0.2% Triton X-100 for 5 min, followed by incubation with mouse monoclonal anti-Myc or anti-HA antibody (1:200 dilution) for 1 h. After three washes with PBS, cells were stained with Texas Red-conjugated anti-mouse IgG secondary antibody and DAPI for another 1 h. Microscopy was similarly performed as reported previously (26). To quantify the nuclear distribution of ATF2 mutants in Fig. 5, COS-1 cells were seeded on coverslips and co-transfected with indicated plasmids and pHA-Venus for 16 h. After performing Myc and DAPI staining, the coverslips were mounted on glass slides with Vectashield Hard Set mounting medium (Vector Laboratories, Burlingame, CA). Venus fluorescent signal was used to define the region of the whole cell body. The percentage of nucleus-localized ATF2 in each individual cell was calculated as (integrated intensity of Myc signal in the nucleus/integrated intensity of Myc signal in the whole cell body) × 100%. Results were presented as means ± S.E. quantified from more than 60 cells.

*UV Irradiation*—COS-1 cells expressing ATF2(LZ-NES3A)-Venus were irradiated with UVC (120 J/m$^2$) in a Spectrolinker XL-1000 UV cross-linker (Spectronic Corp.). Cells were harvested at the indicated time points and subjected to Western blot with anti-phospho-ATF2 antibody. The phosphorylation status of the exogenous ATF2 was quantified by ImageJ software.

*Statistical Analysis*—The data were expressed as means ± S.E. and analyzed by GraphPad Prism 5 (La Jolla, CA). Student's *t* test was used to determine the difference between two groups. For multiple-group comparisons, data were analyzed by one-way analysis of variance, followed by Tukey post-test if significant differences were found.

## RESULTS

*N-terminal Domain Promotes ATF2 Nuclear Export in CRM1-dependent Manner*—We previously demonstrated that ATF2 contains an NES in the leucine zipper region (termed LZ-NES), which, in conjunction with two NLSs in the basic region, regulates ATF2 nucleocytoplasmic shuttling (Fig. 1*A*). We also observed that deletion of the NTD (residues 1–341) of ATF2 increased nuclear localization of Jun-ATF2 heterodimers (33), whereas overexpressed full-length ATF2 was predominantly localized in the cytoplasm despite possession of the two NLS motifs (19). These results suggest that the NTD of ATF2 may negatively regulate ATF2 nuclear localization. To test this possibility, we examined the effect of an NTD deletion on ATF2 subcellular localization. Wild-type and NTD-deleted ATF2 were expressed as fusion proteins with a monomeric form (A206K mutant) of the fluorescent protein Venus in COS-1 cells. As shown in Fig. 1*B*, deletion of the NTD alone resulted in a predominant nuclear localization, demonstrating that the NTD does play a negative role in the nuclear localization of ATF2. To determine the subcellular localization of the NTD, we expressed ATF2(1–341) as a fusion with Venus(A206K) and observed that ATF2(1–341)-Venus(A206K) was predominantly localized in the cytoplasm (Fig. 1*B*). This result suggests that the NTD of ATF2 may possess a cytoplasmic localization activity. Interestingly, treatment of cells with LMB, a CRM1-specific nuclear export inhibitor (34), significantly increased the nuclear localization of ATF2(1–341)-Venus(A206K) (Fig. 1*C*). Thus, predominant cytoplasmic localization of the ATF2 NTD is probably mediated by a CRM1-dependent nuclear export mechanism. To determine whether the nuclear export activity conferred by the NTD is sufficient to drive ATF2 export, we tested the effect of LMB on the localization of ATF2(LZ-NES3A), a previously identified LZ-NES mutant ($^{405}$VAQLKQLLL$^{413}$ to $^{405}$VAQAKQALA$^{413}$) (19). As we

Downloaded from www.jbc.org at Purdue University Libraries, on September 24, 2012

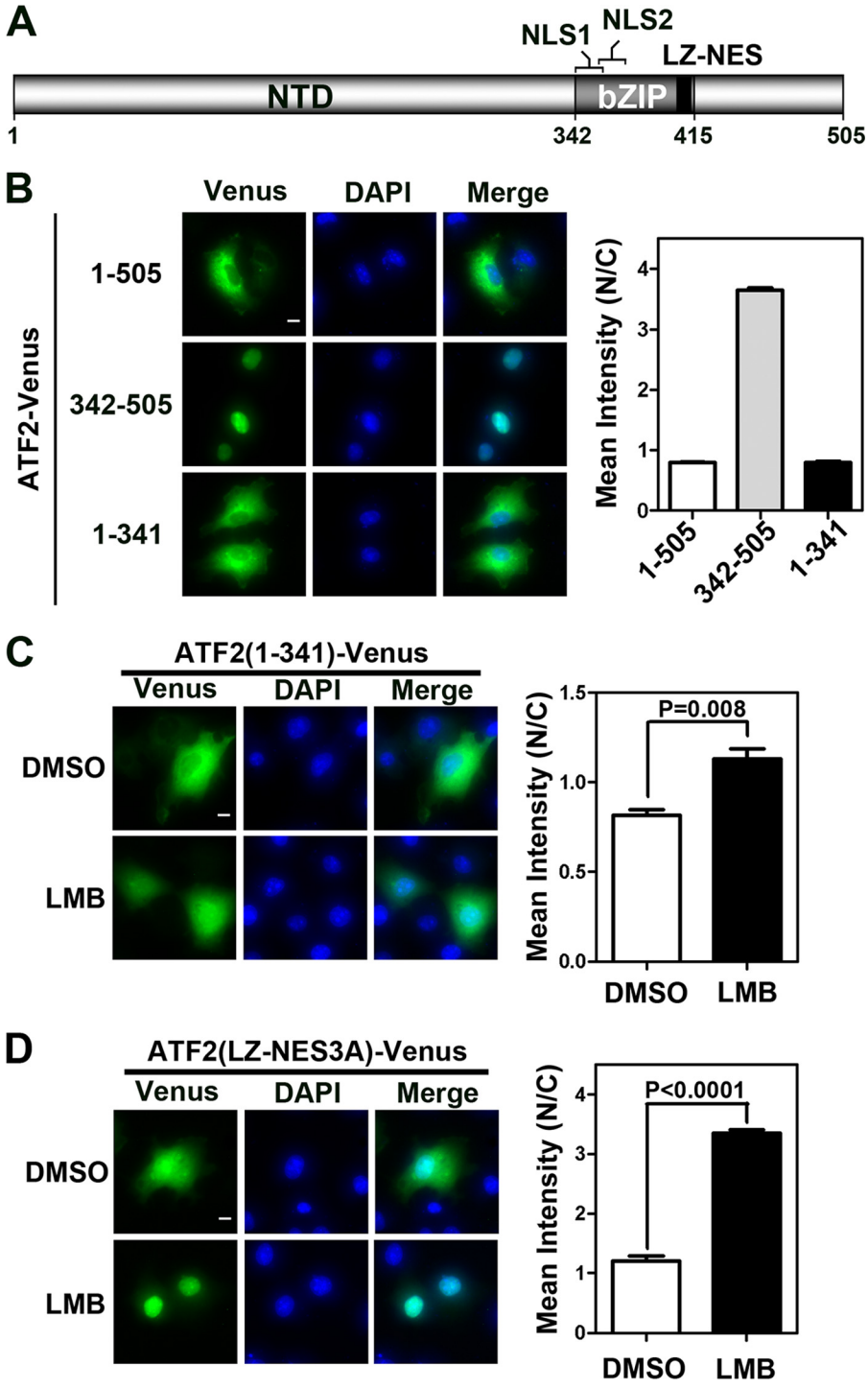


FIGURE 1. **The N-terminal domain contributes to CRM1-dependent nuclear export of ATF2.** *A*, schematic representation of previously identified NLS and NES motifs in ATF2. Two NLSs (NLS1 (residues 342–353) and NLS2 (residues 356–372)) are in the basic region, and one NES (*black box*; residues 405–413) is located in the leucine zipper region. *B*, subcellular localization of the indicated ATF2-Venus(A206K) fusion proteins. COS-1 cells were transfected with plasmids encoding FLAG-ATF2(1–505)-Venus(A206K) (full-length ATF2), FLAG-ATF2(342–505)-Venus(A206K), or FLAG-ATF2(1–341)-Venus(A206K) for 16 h. *Left*, representative images acquired after the cells were fixed, permeabilized, and stained with DAPI. *Scale bar*, 10 $\mu$m. *Right*, quantitative results of the ratio of nuclear to cytoplasmic fluorescence intensity from three independent experiments. *C*, effect of LMB on subcellular localization of ATF2(1–341)-Venus(A206K). COS-1 cells were transfected with the plasmid encoding FLAG-ATF2(1–341)-Venus(A206K) for 14 h, followed by LMB (20 ng/ml) or DMSO treatment for 3.5 h. *Left*, representative images. *Scale bar*, 10 $\mu$m. *Right*, quantitative results of the ratio of nuclear to cytoplasmic fluorescence intensity from three independent experiments. *D*, effect of LMB on subcellular localization of ATF2(LZ-NES3A)-Venus(A206K). COS-1 cells were transfected with the plasmid encoding FLAG-ATF2(LZ-NES3A)-Venus(A206K) for 14 h, followed by LMB or DMSO treatment for 3.5 h. *Left*, representative images. *Scale bar*, 10 $\mu$m. *Right*, quantitative results of the ratio of nuclear to cytoplasmic fluorescence intensity from three independent experiments. *Error bars*, S.E.

observed previously (19), mutation of LZ-NES significantly increased nucleus-localized ATF2 (Fig. 1*D*). Interestingly, treatment of cells with LMB further sequestered ATF2(LZ-NES3A) in the nucleus. Taken together, these results suggest that the ATF2 NTD may possess an additional CRM1-dependent nuclear export activity.

Downloaded from www.jbc.org at Purdue University Libraries, on September 24, 2012

*ATF2 NTD Does Not Contain Canonical NES*—To determine whether the NTD has any NES motifs, we searched the N-terminal 341 residues of ATF2 using Net NES1.1 (35). We also manually compared the amino acid sequence within the NTD against the canonical NES sequence $\Phi^1X_{2-3}\Phi^2X_{2-3}\Phi^3X\Phi^4$ (where Φ represents Leu, Ile, Val, Phe, or Met, and *X* is any amino acid) (35, 36). These searches identified four putative NES motifs: PNES1, PNES2, PNES3, and PNES4 (Fig. 2*A*). To determine if these motifs are functional NESs, we mutated the conserved hydrophobic residues (shown in *boldface type* in Fig. 2*A*) within each putative NES to alanines in the context of ATF2(LZ-NES3A). As shown in Fig. 2, *B* and *C*, all of these mutations did not increase the nuclear localization of ATF2(LZ-NES3A) in the absence of LMB, whereas LMB treatment still sequestered the mutant fusions in the nucleus. Moreover, ATF2(PNES1–4m, LZ-NES3A)-Venus(A206K), a mutant with all four putative NESs and LZ-NES mutated, remained responsive to LMB. These results suggest that these four putative NES motifs in the NTD do not confer the CRM1-dependent nuclear export activity of ATF2 and that they are not functional NESs.

*Residues 1–73 of ATF2 Contain Sequence Required for CRM1-dependent Nuclear Export*—Because mutation analysis suggested that the ATF2 NTD does not possess a canonical NES, we then made an N-terminal truncation and a series of internal deletions in the NTD to map the region responsible for mediating the CRM1-dependent nuclear export. To exclude the potential impact of LZ-NES on ATF2 subcellular localization, all of these mutants were generated in the context of ATF2(LZ-NES3A) (Fig. 3*A*). As shown in Fig. 3, *B* and *C*, ATF2(Δ1–73, LZ-NES3A)-Venus(A206K) was almost completely localized in the nucleus, whereas other ATF2 mutants did not show any significant increase in the nuclear localization. Importantly, LMB treatment further increased the nuclear localization of all other ATF2 mutants but not ATF2(Δ1–73, LZ-NES3A)-Venus(A206K). These results suggest that the first 73 residues of ATF2 contribute to the CRM1-dependent nuclear export of ATF2 NTD. Consistent with this notion, the ATF2(1–341) fragment only was predominantly localized in the cytoplasm, whereas the ATF2(74–341) fragment was distributed in both the nucleus and the cytoplasm (supplemental Fig. 2).

*Identification of Non-canonical NES in Most N-terminal End of ATF2*—To confirm that the first 73 residues of ATF2 may contain an autonomous NES, we fused ATF2(1–73) to the N terminus of 2xVenus(A206K). The fusion to two Venus proteins increases the molecular mass (to ~65 kDa) of the fusion protein and thus attenuates its passive diffusion rate across the nuclear pore complex. Similar strategies have been utilized by others to evaluate NES activity (37–39). As shown in Fig. 4*A*, ATF2(1–73)-2xVenus(A206K) was predominantly localized in the cytoplasm. Importantly, treatment of cells with LMB altered its predominant cytoplasmic localization and increased its localization in the nucleus, reinforcing our hypothesis that a CRM1-dependent NES resides in this region. Because canonical NES is a hydrophobic residue-enriched motif, we then searched for hydrophobic residue-enriched regions within the first 73 residues and identified $^1$MKFKLHV$^7$ (termed N-NES) as the only potential hydrophobic stretch. Although this sequence does not match the consensus NES, a similar atypical NES has been reported in Eps15 (40) (Fig. 4*B*). To determine if the hydrophobic stretch functions as an NES, we mutated the four hydrophobic residues to alanines (N-NES4A: $^1$MKFKLHV$^7$ to $^1$AKAKAHA$^7$) in ATF2(1–73). As shown in Fig. 4*B*, transiently expressed ATF2(1–73, N-NES4A)-2xVenus(A206K) was distributed throughout the cell, suggesting that the hydrophobic residues in the most N-terminal end of ATF2 may function as an NES. We also confirmed that the N-NES is functional in other cell lines, including HEK 293T, LNCaP, and PC3 cells (supplemental Fig. 3). To determine that this atypical NES can be recognized by CRM1, we performed a co-IP assay to verify the interaction between CRM1 and ATF2(1–341). We coexpressed Myc-CRM1 and FLAG-Venus(A206K)-ATF2(1–341) or FLAG-Venus(A206K)-ATF2(1–341, N-NES4A) in COS-1 cells and then performed co-IP with anti-FLAG antibody. The insertion of Venus between FLAG and ATF2 is to avoid masking of the FLAG epitope when CRM1 binds to the NTD of ATF2. We found that Myc-CRM1 was efficiently co-immunoprecipitated with FLAG-Venus(A206K)-ATF2(1–341) but not FLAG-Venus(A206K)-ATF2(1–341, N-NES4A) (Fig. 4*C*), suggesting that the hydrophobic stretch $^1$MKFKLHV$^7$ is recognized and bound by CRM1.

To examine the impact of N-NES on ATF2 subcellular localization, we introduced the mutations into ATF2 in the context of full-length ATF2 and determined the localization of ATF2. Mutation of N-NES significantly increased nuclear distribution of ATF2, indicating that N-NES does regulate the subcellular localization of ATF2 (Fig. 4*D*). Importantly, ATF2 was predominantly localized in the nucleus when both N-NES and LZ-NES were mutated. Moreover, LMB treatment did not further increase the nuclear localization of this mutant (supplemental Fig. 4), suggesting that no additional CRM1-dependent NES exists in ATF2. Function of N-NES in full-length ATF2 was also confirmed in HEK 293T and LNCaP cells, albeit N-NES seems to be a dominant export signal in both cell types (supplemental Figs. 5 and 6). Taken together, these results demonstrate that both NESs contribute to the nuclear export of ATF2 and suggest that a complete nuclear localization of ATF2 may require functional inactivation of both NESs.

*Transcriptional Activity of ATF2 Is Negatively Regulated by N-NES*—We previously demonstrated that the lack of transcriptional activity of exogenously expressed ATF2 is probably due to the predominant cytoplasmic localization of overexpressed ATF2 (19). The increase in nuclear localization of N-NES-disrupted ATF2 prompted us to examine if its transcriptional activity is enhanced. We similarly used the *jun2* luciferase reporter gene to examine the ATF2 transcriptional activity (9, 19, 41). Consistent with our previous observation (19), wild-type ATF2 barely activated the *jun2-luc* reporter (Fig. 5*A*). Interestingly, ~3-fold activation of *jun2-luc* by ATF2(N-NES4A) was observed. On the contrary, ATF2 with mutations in LZ-NES or both NESs did not activate the *jun2-luc* reporter. Because LZ-NES of ATF2 spans between the fourth and fifth heptad of the leucine zipper region and replacement of the leucine in the fourth heptad (corresponding to

Downloaded from www.jbc.org at Purdue University Libraries, on September 24, 2012

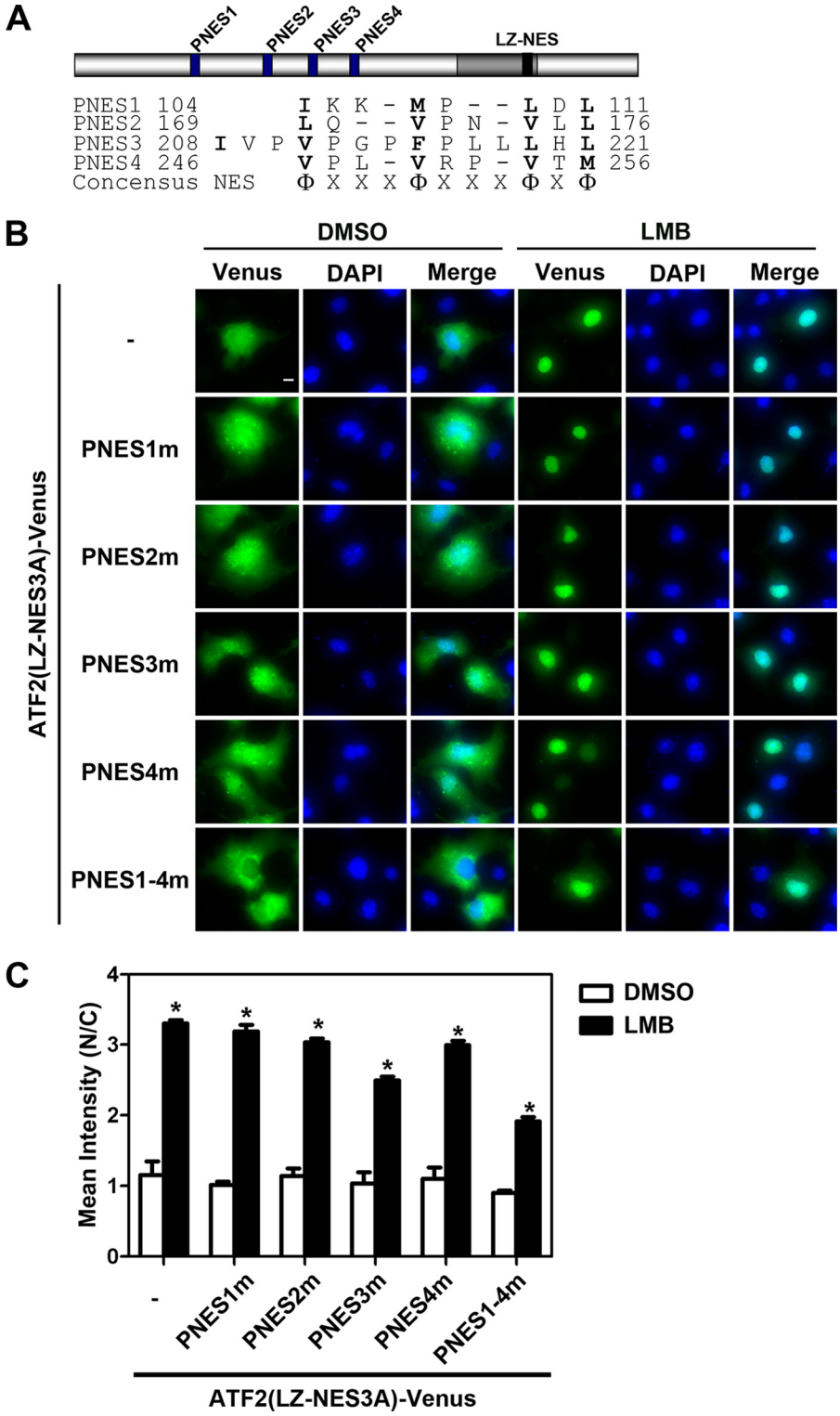


FIGURE 2. **ATF2 NTD does not contain a canonical NES.** *A*, schematic representation of four putative NESs identified in the ATF2 NTD. The amino acids shown in *boldface type* are hydrophobic residues that match the consensus NES. *B*, effects of LMB on subcellular localization of putative NES-mutated ATF2(LZ-NES3A)-Venus(A206K). The hydrophobic residues (shown in *boldface type* in *A*) of each (PNES1m, PNES2m, PNES3m, and PNES4m) or all putative NESs (PNES1–4m) were replaced with alanines in the context of ATF2(LZ-NES3A)-Venus(A206K). COS-1 cells were transfected with plasmids encoding the indicated C-terminal Venus(A206K)-fused proteins for 14 h, followed by LMB or DMSO treatment for 3.5 h. Shown are representative images. *Scale bar*, 10 $\mu$m. *C*, quantification of the results in *B*. Shown is the ratio of nuclear to cytoplasmic fluorescence intensity from three independent experiments. *Asterisks* indicate a significant difference ($p < 0.05$) when compared with the respective DMSO treatment group. *Error bars*, S.E.

the Leu-408 of ATF2) with alanine was shown to reduce the stability of leucine-zipper dimer (42, 43), we tested if LZ-NES3A mutation affects heterodimerization of ATF2 and c-Jun, the complex binding to the *jun2* response element (44). A co-IP was used to determine if this mutation affects the binding of exogenous ATF2 to endogenous c-Jun. HEK

Downloaded from www.jbc.org at Purdue University Libraries, on September 24, 2012

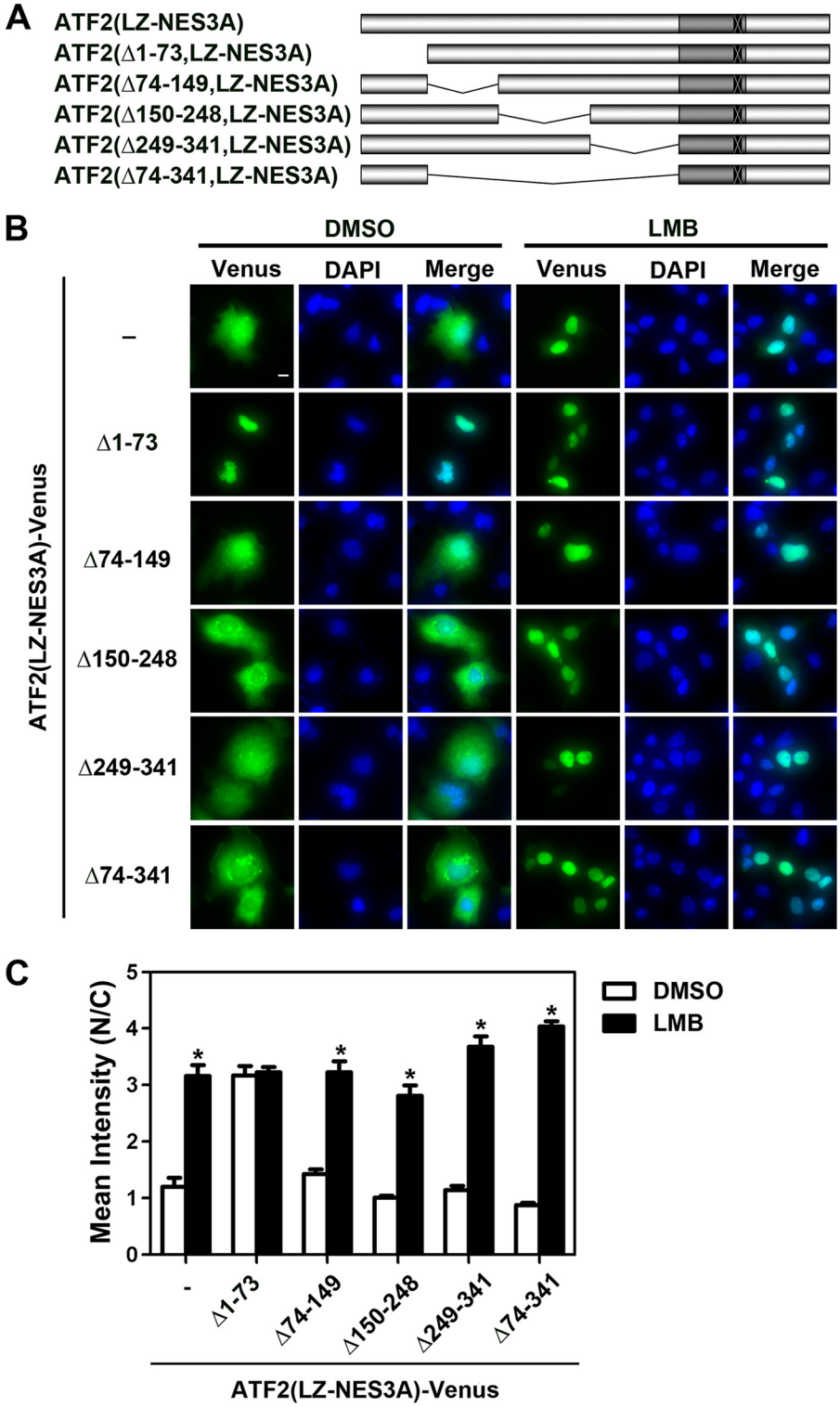


FIGURE 3. **N-terminal 73 residues of ATF2 confer the CRM1-dependent nuclear export activity.** *A*, schematic view of N-terminal truncation and various internal deletion mutants used for mapping the NES within the NTD of ATF2. *B*, effects of LMB on subcellular localization of ATF2(LZ-NES3A)-Venus(A206K) mutants in which various regions within NTD were deleted. COS-1 cells were transfected with plasmids encoding the indicated C-terminal Venus(A206K)-fusion proteins for 14 h, followed by LMB or DMSO treatment for 3.5 h. Shown are representative images. *Scale bar*, 10 $\mu$m. *C*, quantification of the results in *B*. Shown is the ratio of nuclear to cytoplasmic fluorescence intensity (*N/C*) from three independent experiments. *, significant difference ($p < 0.05$) when compared with the respective DMSO treatment group. *Error bars*, S.E.

293T cells were used due to the high transfection efficiency, which allowed us to efficiently co-immunoprecipitate endogenous c-Jun. As shown in Fig. 5*B*, LZ-NES3A mutation reduced the interaction between ATF2 and c-Jun, suggesting that the stability of ATF2·c-Jun complex is essential for its transcriptional activity.

We next sought to confirm that the subcellular localization of these ATF2 proteins is similar to that of Venus-fused ones.

Downloaded from www.jbc.org at Purdue University Libraries, on September 24, 2012

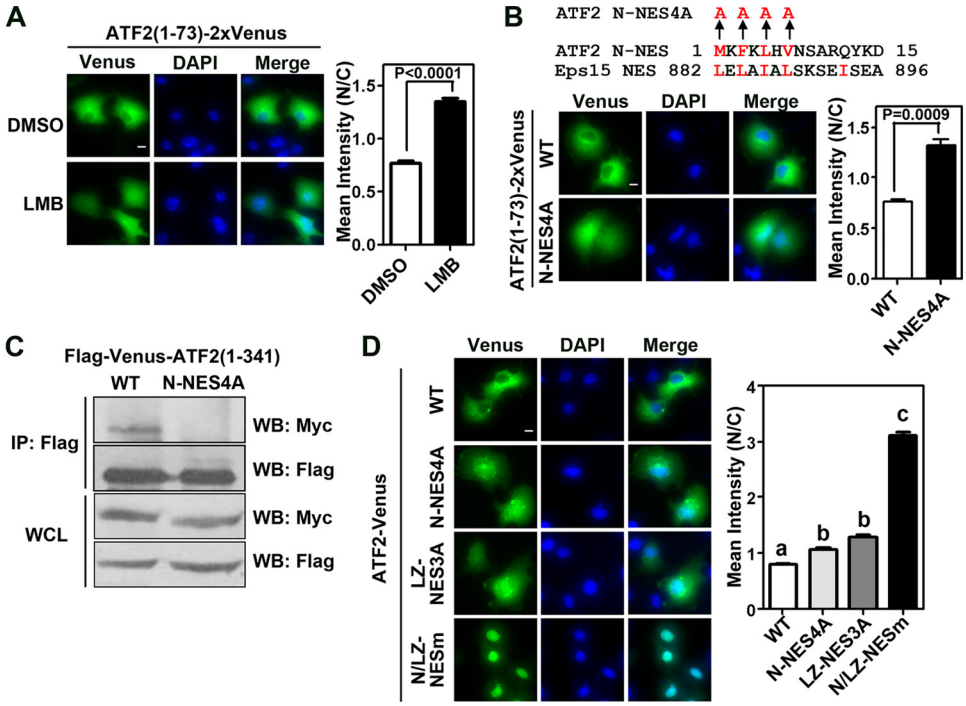


FIGURE 4. **Identification of an NES in the most N-terminal end of ATF2.** *A*, effect of LMB on subcellular localization of ATF2(1–73)-2xVenus(A206K). COS-1 cells were transfected with the plasmid encoding FLAG-ATF2(1–73)-2xVenus(A206K) for 14 h, followed by LMB or DMSO treatment for 3.5 h. *Left*, representative images. *Scale bar*, 10 $\mu$m. *Right*, quantitative results from three independent experiments. *B*, effect of N-NES mutation on subcellular localization of ATF2(1–73)-2xVenus(A206K). *Top*, alignment of the first 15 residues of ATF2 with the identified NES in Eps15. The hydrophobic residues (*red letters*) were replaced with alanines in ATF2 to make the N-NES4A mutant. COS-1 cells were transfected with plasmids encoding FLAG-ATF2(1–73)-2xVenus(A206K) or FLAG-ATF2(1–73, N-NES4A)-2xVenus(A206K) for 16 h. *Bottom left*, representative images. *Scale bar*, 10 $\mu$m. *Bottom right*, quantitative results from three independent experiments. *C*, interaction of CRM1 with ATF2 N-NES in COS-1 cells. COS-1 cells were co-transfected with plasmids encoding Myc-CRM1 and FLAG-Venus(A206K)-ATF2(1–341) or FLAG-Venus(A206K)-ATF2(1–341, N-NES4A). Whole cell lysate (*WCL*) was immunoprecipitated with anti-FLAG antibody. The immunoprecipitates were examined by Western blot (*WB*) using anti-Myc antibody. Similar levels of exogenous protein expression were confirmed by subjecting 4% of whole cell lysate to Western blot. Shown is a representative co-IP result from three independent experiments. *D*, effect of NES mutations on subcellular localization of full-length ATF2-Venus(A206K). COS-1 cells were transfected with plasmids encoding FLAG-ATF2(WT)-Venus(A206K), FLAG-ATF2(N-NES4A)-Venus(A206K), FLAG-ATF2(LZ-NES3A)-Venus(A206K), or FLAG-ATF2(N/LZ-NESm)-Venus(A206K) for 16 h. *Left*, representative images. *Scale bar*, 10 $\mu$m. *Right*, quantitative results from three independent experiments. *Different letters above* the *bars* indicate significant differences ($p < 0.05$) in the ratio of nuclear to cytoplasmic fluorescence intensity (one-way analysis of variance). *Error bars*, S.E.

To avoid the potential masking of FLAG epitope by the CRM1/N-NES interaction, we fused a Myc tag to the C-terminal end of each protein and determined the percentage of nucleus-localized ATF2 mutants by immunostaining with anti-Myc antibody. As shown in Fig. 5*C*, mutation of N-NES increased the nuclear distribution of ATF2 from 14 to 37%, whereas mutation of both NESs further brought the percentage of ATF2 in the nucleus up to 79%. We then performed the same reporter assay and found that mutation of N-NES also significantly enhanced transcriptional activity of the ATF2-Myc fusion protein, albeit to a lesser extent when compared with the counterpart without Myc tag (supplemental Fig. 7). In summary, these results suggest that N-NES negatively regulates ATF2 nuclear localization and the transcriptional activity.

*N-NES Is Not Regulated by MAPK Phosphorylation*—Transcriptional activity of ATF2 is regulated by MAPKs, which phosphorylate Thr-69/71 in the NTD. We previously demonstrated that MAPK phosphorylation did not affect the subcellular localization of full-length ATF2 with intact N-NES and LZ-NES (19). To determine whether MAPK-mediated phosphorylation has any impact on N-NES, we substituted Thr-69 and -71 with non-phosphorylatable alanine, phosphomimic aspartic acid, or glutamic acid in the background of ATF2(LZ-NES3A). As shown in Fig. 6*A*, none of the substitutions altered the subcellular localization of ATF2. We also found that the exogenous ATF2(LZ-NES3A)-Venus(A206K) but not the alanine mutant was readily phosphorylated at Thr-71 in cells (Fig. 6*B*). To further evaluate the effect of ATF2 Thr-69/Thr-71 phosphorylation on N-NES activity, COS-1 cells expressing ATF2(LZ-NES3A)-Venus(A206K) were subjected to UV irradiation, which induces ATF2 phosphorylation by activating JNK and p38 kinases (9, 12, 45). No significant change in subcellular localization of the exogenous ATF2 was observed (Fig. 6*C*), although UV irradiation indeed enhanced ATF2 phosphorylation (Fig. 6*D*). Taken together, these results indicate that the N-NES is unlikely to be regulated by MAPK-mediated phosphorylation.

## DISCUSSION

We previously demonstrated that ATF2 possesses two NLS and one NES (LZ-NES) and constitutively shuttles between the cytoplasm and nucleus in a monomeric form (19). In the present study, we identified another NES (N-NES) in the most N-terminal end of ATF2, suggesting that the subcellular localization of ATF2 is modulated by multiple layers of regulations. Nuclear localization of ATF2 requires formation of a heterodimer with c-Jun, which masks the LZ-NES of ATF2 and anchors ATF2 in the nucleus. With limited c-Jun protein, ATF2

Downloaded from www.jbc.org at Purdue University Libraries, on September 24, 2012

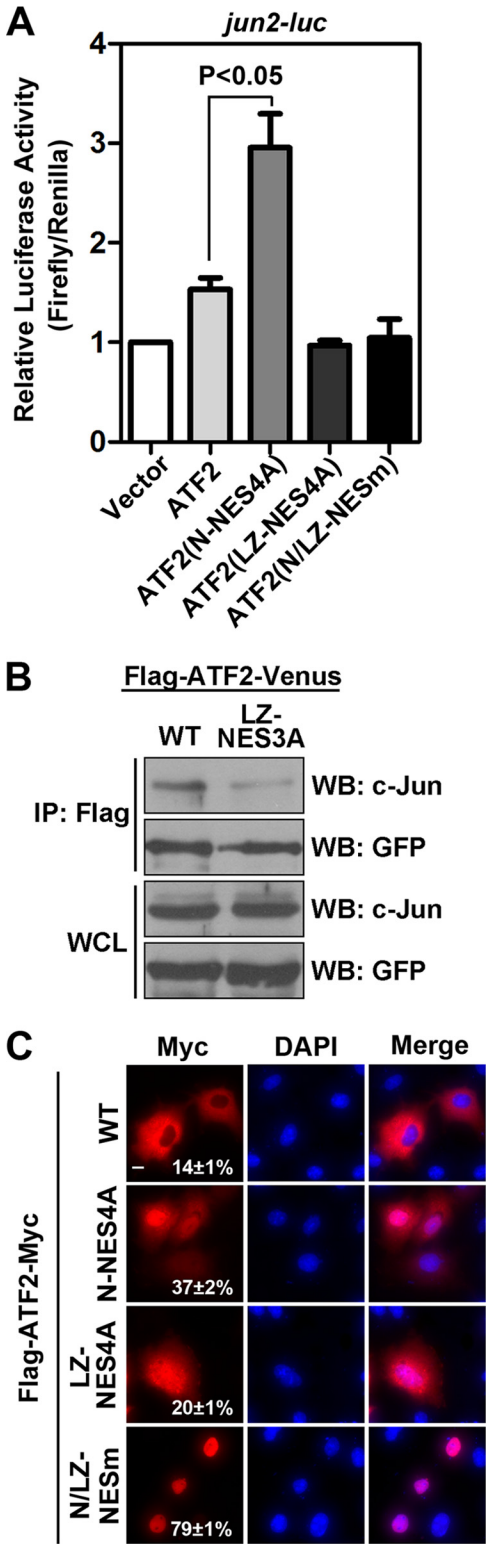


FIGURE 5. **Mutation of N-NES enhanced ATF2 transcriptional activity.** *A*, effect of NES mutations on transcriptional activity of ATF2. Serum-starved COS-1 cells were transfected with 0.5 $\mu$g of *jun2-luc*, 100 ng of pRL-TK along with 2 $\mu$g of pCMV-FLAG (vector), pFLAG-ATF2, pFLAG-ATF2(N-NES4A), pFLAG-ATF2(LZ-NES3A), or pFLAG-ATF2(N/LZ-NESm) for 24 h. Values of firefly/*Renilla* luciferase were presented as fold change over vector control. Results are shown as mean ± S.E. from three independent experiments done in duplicate. *B*, effect of LZ-NES mutation on ATF2·c-Jun heterodimerization. HEK 293T cells were transfected with plasmids encoding FLAG-ATF2-Venus(A206K) or FLAG-ATF2(LZ-NES3A)-Venus(A206K). Whole cell lysate (*WCL*) was immunoprecipitated with anti-FLAG antibody followed by Western blot (*WB*) analysis with anti-c-Jun antibody. Similar levels of exogenous protein expression were confirmed by subjecting 2% of whole cell lysate to Western blotting with anti-GFP antibody, which recognizes Venus. Shown is a representative co-IP result from two independent experiments. *C*, effect of NES mutations on subcellular localization of ATF2-Myc fusion proteins. COS-1 cells were transfected with pHA-Venus along with plasmids encoding FLAG-ATF2-Myc, FLAG-ATF2(N-NES4A)-Myc, FLAG-ATF2(LZ-NES3A)-Myc, or FLAG-ATF2(N/LZ-NESm)-Myc for 16 h. Cells were then fixed and subjected to immunostaining with anti-Myc antibody. *Scale bar*, 10 $\mu$m. The number indicates the percentage of nuclear distribution ± S.E. quantified from more than 60 cells. *Error bars*, S.E.

is predominantly located in the cytoplasm due to two mechanisms. First, ATF2 homodimerization in the cytoplasm can inhibit nuclear import (19). Second, localization of the ATF2 monomer is determined by the balance between N-NES, LZ-NES, and two NLSs. The nuclear export rate contributed by both N-NES and LZ-NES seems to outweigh the nuclear import rate conferred by the two NLSs because the homodimerization-deficient mutant ATF2(L4P) is predominantly located in the cytoplasm (19).

Since identification of the consensus NES motifs (36), many nucleocytoplasmic shuttling proteins have been demonstrated to possess the canonical NES motif. The NES motif is a hydrophobic-rich region, defined as $\Phi^1X_{2-3}\Phi^2X_{2-3}\Phi^3X\Phi^4$ (where $\Phi$ represents Leu, Ile, Val, Phe, or Met, and $X$ is any amino acid) (35, 36). Interestingly, only 72% of reported NES motifs match this well defined consensus NES (35), and the remaining motifs have only partially conserved NESs. As presented in this study, the N-NES of ATF2, MKFKLHV, has only one amino acid residue between $\Phi^1/\Phi^2$ and $\Phi^2/\Phi^3$, respectively. Because similar sequence presented in Eps15 acts as a functional NES (40), we have provided several lines of evidence to demonstrate that the N-NES is also functional. First, the N-terminal 73 residues are sufficient to render a tandem Venus fusion to be localized in the cytoplasm (Fig. 4*A*). Second, this tandem Venus fusion is responsive to LMB treatment. Third, mutation of N-NES in the context of full-length ATF2 increased ATF2 nuclear localization (Fig. 4*D*). Finally, CRM1 can be coimmunoprecipitated with the wild-type N-terminal domain of ATF2 but not the mutant form (Fig. 4*C*). Thus, ATF2 has a canonical NES in its leucine zipper domain and a non-canonical NES in the most N-terminal end.

The N-terminal end localization of N-NES may allow it to be more accessible to CRM1 (46). Interestingly, due to its unique location, a careful experimental design is needed in order to determine ATF2 subcellular localization. We observed that an N-terminal FLAG tag immediately adjacent to the N-NES prevented us from staining the nucleus-localized FLAG-ATF2 (data not shown), which is probably due to the binding of CRM1 to the N-NES of FLAG-ATF2 in the nucleus. Similarly, we also observed a slight but significant increase in nuclear localization of ATF2 when Venus is fused to the N terminus of the protein (supplemental Fig. 8), which may be due to a steric hindrance for the CRM1/N-NES interaction. Therefore, C-terminal fluorescent protein or tag fusions are preferred when exogenous ATF2 fusion proteins are used for the analysis of ATF2 subcellular localization.

Nucleocytoplasmic shuttling of transcription factors has emerged as an important research area. Many transcription fac-

Downloaded from www.jbc.org at Purdue University Libraries, on September 24, 2012

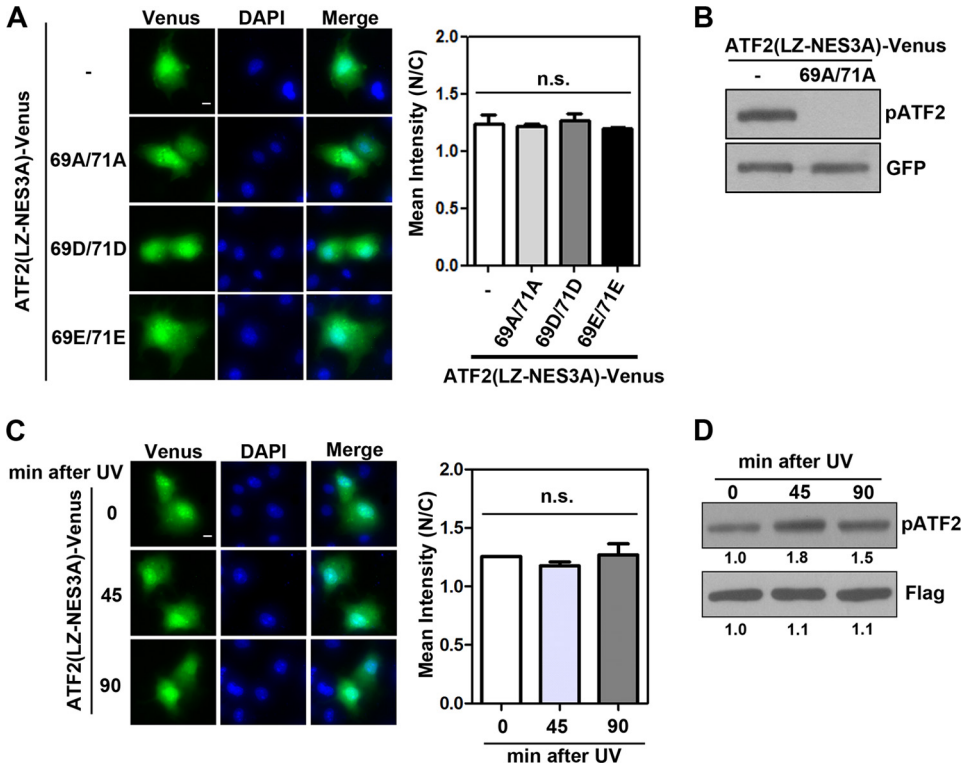


FIGURE 6. **N-NES of ATF2 is not regulated by MAPK phosphorylation.** *A*, effect of various Thr-69/Thr-71 mutants on subcellular localization of ATF2(LZ-NES3A)-Venus(A206K). COS-1 cells were transfected with plasmids encoding indicated mutant ATF2 fused to Venus for 16 h. *Left*, representative images. *Scale bar*, 10 $\mu$m. *Right*, quantitative results of the ratio of nuclear to cytoplasmic fluorescence intensity from three independent experiments. No significant difference was found (*n.s.*; one-way analysis of variance). *B*, effect of T69A/T71A mutation on Thr-71 phosphorylation status of ATF2(LZ-NES3A)-Venus(A206K). COS-1 cells were transfected with plasmids encoding FLAG-ATF2(LZ-NES3A)-Venus(A206K) or FLAG-ATF2(T69A,T71A,LZ-NES3A)-Venus(A206K) for 16 h. Thr-71 phosphorylation status was examined by Western blot. Comparable expression of both exogenous proteins was confirmed by immunoblotting with anti-GFP antibody. *C*, effect of UV irradiation on subcellular localization of ATF2(LZ-NES3A)-Venus(A206K). COS-1 cells were transfected with the plasmid encoding FLAG-ATF2(LZ-NES3A)-Venus(A206K) for 16 h followed by UV irradiation (120 J/m$^2$). Cells were fixed at 45 or 90 min after treatment. *Left*, representative images. *Scale bar*, 10 $\mu$m. *Right*, quantitative results of the ratio of nuclear to cytoplasmic fluorescence intensity from three independent experiments. No significant difference was found (one-way analysis of variance). *D*, effect of UV irradiation on Thr-71 phosphorylation status of ATF2(LZ-NES3A)-Venus(A206K). Thr-71 phosphorylation status of ATF2(LZ-NES3A)-Venus(A206K) at the indicated time point after UV treatment was determined by Western blot. The *number below* each *lane* is the quantified fold change when compared with the *first lane*. *Error bars*, S.E.

tors critical to cell fate determination are tightly regulated by multiple NLS and NES motifs. This may allow regulation of these transcription factors by multiple mechanisms. For example, p53 contains two NESs and three NLSs (47–50). The N-terminal NES is regulated by phosphorylation events in response to DNA damage (50), whereas the NES in the tetramerization domain is masked upon p53 oligomerization (49). In the case of ATF2, we have shown that the function of LZ-NES is inhibited when ATF2 heterodimerizes with the Jun family proteins. However, it is currently unknown whether and how the N-NES of ATF2 is regulated. Because phosphorylation at Thr-69 and Thr-71 by MAPKs is known to stimulate transactivation activity of ATF2, we initially thought that MAPK phosphorylation may regulate ATF2 subcellular localization. However, it does not appear to be the case because substitutions of these two residues to non-phosphorylatable alanines or phosphorylation-mimicking aspartic acid or glutamic acid residues did not affect the localization of ATF2(LZ-NES3A) (Fig. 6*A*). In addition, further induction of phosphorylation at these two residues by UV did not affect the localization of this mutant (Fig. 6*C*). Because ATF2 is also phosphorylated at other sites in the NTD (51, 52), it remains to be investigated whether phosphorylation of these additional sites regulates the activity of N-NES. Interestingly, mutation of LZ-NES increased nuclear localization of ATF2 in COS-1 cells but not in HEK 293T or LNCaP cells, suggesting that N-NES is a dominant export signal in the latter two cell types. One possible explanation is that N-NES activity is enhanced by signaling that is activated in these cell types. In this case, comparing the difference of cellular signaling between cell types with differential N-NES activity may help unravel mechanisms that regulate N-NES. Alternatively, activity of N-NES may be modulated by ATF2-interacting proteins, such as E1A and CREB-binding protein (21). Also, undifferentiated embryonic cell transcription factor 1 (UTF1) (53) and activating signal cointegrator-2 (ASC-2) (54) are reported to bind the NTD of ATF2 and function as coactivators. It will be interesting to test if these coactivators enhance ATF2 transcriptional activity by masking N-NES and anchoring ATF2 in the nucleus.

Our results showed that mutation of N-NES enhanced transcriptional activity of FLAG-ATF2 and FLAG-ATF2-Myc by ~90 and 30%, respectively (Fig. 5 and supplemental Fig. 7). Because C-terminal Myc tag does not appear to affect ATF2 stability (data not shown), it may reduce the transcriptional potential of ATF2 by causing a conformational change. Indeed, it has been reported that function of transcription factors can be affected by N- or C-terminal tags (55, 56). Nevertheless, the

Downloaded from www.jbc.org at Purdue University Libraries, on September 24, 2012

enhanced reporter gene activation by ATF2 with mutations in the N-NES correlates with its increased nuclear localization, suggesting that regulation of N-NES by itself could increase the transcriptional activity of ATF2. In this sense, it is worth noting that there are multiple ATF2 alternative spliced variants that have been deposited to the NCBI database, although their functions remain largely uninvestigated. For example, ATF2-Var13 (GenBank™ number AAY17215.1) lacks the N-terminal 18 residues due to the loss of exon 3, where N-NES is located. Based on our finding here, it is very likely that the transcriptional activity of ATF2-Var13 may be less subject to the regulation by its subcellular localization. Therefore, a switch between spliced variants may be an alternative mechanism to regulate ATF2 subcellular localization and its activity. Consistent with this notion, alignment of full-length ATF2 with those from several species reveals that N-NES is only present in *Homo sapiens*, *Canis familiaris*, and *Bos taurus* ATF2 and not in *Gallus gallus*, *Mus musculus*, *Rattus norvegicus*, and *Xenopus laevis* (supplemental Fig. 9). It is therefore possible that this additional NES is evolutionarily acquired to deal with more complex regulatory mechanisms in higher organisms. Given that alteration of ATF2 subcellular localization has been observed in several human diseases (22–26), further analysis of the regulation of N-NES under these pathological conditions will probably provide exciting insight into the role of ATF2 in the pathogenesis of human diseases.

*Acknowledgments—We thank Christopher Suarez for critically reading the manuscript. DNA sequencing was conducted in the Purdue University Center for Cancer Research Genomic Core Facility, supported by National Institutes of Health, NCI, Grant CCSG CA23168 (to the Purdue University Center for Cancer Research).*

## REFERENCES

1. Wagner, E. F. (2001) AP-1. Introductory remarks. *Oncogene* **20,** 2334–2335
2. Hai, T. W., Liu, F., Coukos, W. J., and Green, M. R. (1989) Transcription factor ATF cDNA clones. An extensive family of leucine zipper proteins able to selectively form DNA-binding heterodimers. *Genes Dev.* **3,** 2083–2090
3. Benbrook, D. M., and Jones, N. C. (1990) Heterodimer formation between CREB and JUN proteins. *Oncogene* **5,** 295–302
4. Hai, T., and Curran, T. (1991) Cross-family dimerization of transcription factors Fos/Jun and ATF/CREB alters DNA binding specificity. *Proc. Natl. Acad. Sci. U.S.A.* **88,** 3720–3724
5. Ma, Q., Li, X., Vale-Cruz, D., Brown, M. L., Beier, F., and LuValle, P. (2007) Activating transcription factor 2 controls Bcl-2 promoter activity in growth plate chondrocytes. *J. Cell Biochem.* **101,** 477–487
6. Salameh, A., Galvagni, F., Anselmi, F., De Clemente, C., Orlandini, M., and Oliviero, S. (2010) Growth factor stimulation induces cell survival by c-Jun. ATF2-dependent activation of Bcl-XL. *J. Biol. Chem.* **285,** 23096–23104
7. Shimizu, M., Nomura, Y., Suzuki, H., Ichikawa, E., Takeuchi, A., Suzuki, M., Nakamura, T., Nakajima, T., and Oda, K. (1998) Activation of the rat cyclin A promoter by ATF2 and Jun family members and its suppression by ATF4. *Exp. Cell Res.* **239,** 93–103
8. Beier, F., Lee, R. J., Taylor, A. C., Pestell, R. G., and LuValle, P. (1999) Identification of the cyclin D1 gene as a target of activating transcription factor 2 in chondrocytes. *Proc. Natl. Acad. Sci. U.S.A.* **96,** 1433–1438
9. van Dam, H., Wilhelm, D., Herr, I., Steffen, A., Herrlich, P., and Angel, P. (1995) ATF-2 is preferentially activated by stress-activated protein kinases to mediate c-jun induction in response to genotoxic agents. *EMBO J.* **14,** 1798–1811
10. Livingstone, C., Patel, G., and Jones, N. (1995) ATF-2 contains a phosphorylation-dependent transcriptional activation domain. *EMBO J.* **14,** 1785–1797
11. Ouwens, D. M., de Ruiter, N. D., van der Zon, G. C., Carter, A. P., Schouten, J., van der Burgt, C., Kooistra, K., Bos, J. L., Maassen, J. A., and van Dam, H. (2002) Growth factors can activate ATF2 via a two-step mechanism. Phosphorylation of Thr-71 through the Ras-MEK-ERK pathway and of Thr-69 through RalGDS-Src-p38. *EMBO J.* **21,** 3782–3793
12. Gupta, S., Campbell, D., Dérijard, B., and Davis, R. J. (1995) Transcription factor ATF2 regulation by the JNK signal transduction pathway. *Science* **267,** 389–393
13. Kawasaki, H., Schiltz, L., Chiu, R., Itakura, K., Taira, K., Nakatani, Y., and Yokoyama, K. K. (2000) ATF-2 has intrinsic histone acetyltransferase activity which is modulated by phosphorylation. *Nature* **405,** 195–200
14. Abdel-Hafiz, H. A., Heasley, L. E., Kyriakis, J. M., Avruch, J., Kroll, D. J., Johnson, G. L., and Hoeffler, J. P. (1992) Activating transcription factor-2 DNA-binding activity is stimulated by phosphorylation catalyzed by p42 and p54 microtubule-associated protein kinases. *Mol. Endocrinol.* **6,** 2079–2089
15. Fuchs, S. Y., Xie, B., Adler, V., Fried, V. A., Davis, R. J., and Ronai, Z. (1997) c-Jun $NH_2$-terminal kinases target the ubiquitination of their associated transcription factors. *J. Biol. Chem.* **272,** 32163–32168
16. Fuchs, S. Y., Fried, V. A., and Ronai, Z. (1998) Stress-activated kinases regulate protein stability. *Oncogene* **17,** 1483–1490
17. Li, X. Y., and Green, M. R. (1996) Intramolecular inhibition of activating transcription factor-2 function by its DNA-binding domain. *Genes Dev.* **10,** 517–527
18. Liu, F., and Green, M. R. (1990) A specific member of the ATF transcription factor family can mediate transcription activation by the adenovirus E1a protein. *Cell* **61,** 1217–1224
19. Liu, H., Deng, X., Shyu, Y. J., Li, J. J., Taparowsky, E. J., and Hu, C. D. (2006) Mutual regulation of c-Jun and ATF2 by transcriptional activation and subcellular localization. *EMBO J.* **25,** 1058–1069
20. Duyndam, M. C., van Dam, H., Smits, P. H., Verlaan, M., van der Eb, A. J., and Zantema, A. (1999) The N-terminal transactivation domain of ATF2 is a target for the co-operative activation of the c-jun promoter by p300 and 12S E1A. *Oncogene* **18,** 2311–2321
21. Sano, Y., Tokitou, F., Dai, P., Maekawa, T., Yamamoto, T., and Ishii, S. (1998) CBP alleviates the intramolecular inhibition of ATF-2 function. *J. Biol. Chem.* **273,** 29098–29105
22. Berger, A. J., Kluger, H. M., Li, N., Kielhorn, E., Halaban, R., Ronai, Z., and Rimm, D. L. (2003) Subcellular localization of activating transcription factor 2 in melanoma specimens predicts patient survival. *Cancer Res.* **63,** 8103–8107
23. Bhoumik, A., Fichtman, B., Derossi, C., Breitwieser, W., Kluger, H. M., Davis, S., Subtil, A., Meltzer, P., Krajewski, S., Jones, N., and Ronai, Z. (2008) Suppressor role of activating transcription factor 2 (ATF2) in skin cancer. *Proc. Natl. Acad. Sci. U.S.A.* **105,** 1674–1679
24. Yamada, T., Yoshiyama, Y., and Kawaguchi, N. (1997) Expression of activating transcription factor-2 (ATF-2), one of the cyclic AMP-response element (CRE)-binding proteins, in Alzheimer disease and non-neurological brain tissues. *Brain Res.* **749,** 329–334
25. Ricote, M., García-Tuñón, I., Bethencourt, F., Fraile, B., Onsurbe, P., Paniagua, R., and Royuela, M. (2006) The p38 transduction pathway in prostatic neoplasia. *J. Pathol.* **208,** 401–407
26. Deng, X., Liu, H., Huang, J., Cheng, L., Keller, E. T., Parsons, S. J., and Hu, C. D. (2008) Ionizing radiation induces prostate cancer neuroendocrine differentiation through interplay of CREB and ATF2. Implications for disease progression. *Cancer Res.* **68,** 9663–9670
27. Deng, X., Elzey, B. D., Poulson, J. M., Morrison, W. B., Ko, S. C., Hahn, N. M., Ratliff, T. L., and Hu, C. D. (2011) Ionizing radiation induces neuroendocrine differentiation of prostate cancer cells *in vitro*, *in vivo*, and in prostate cancer patients. *Am. J. Cancer Res.* **1,** 834–844
28. Zacharias, D. A., Violin, J. D., Newton, A. C., and Tsien, R. Y. (2002) Partitioning of lipid-modified monomeric GFPs into membrane microdomains of live cells. *Science* **296,** 913–916

Downloaded from www.jbc.org at Purdue University Libraries, on September 24, 2012

29. Nagai, T., Ibata, K., Park, E. S., Kubota, M., Mikoshiba, K., and Miyawaki, A. (2002) A variant of yellow fluorescent protein with fast and efficient maturation for cell-biological applications. *Nat. Biotechnol.* **20,** 87–90
30. Shaner, N. C., Steinbach, P. A., and Tsien, R. Y. (2005) A guide to choosing fluorescent proteins. *Nat. Methods* **2,** 905–909
31. Ali, S. A., and Steinkasserer, A. (1995) PCR-ligation-PCR mutagenesis. A protocol for creating gene fusions and mutations. *BioTechniques* **18,** 746–750
32. Le, N. H., van der Bent, P., Huls, G., van de Wetering, M., Loghman-Adham, M., Ong, A. C., Calvet, J. P., Clevers, H., Breuning, M. H., van Dam, H., and Peters, D. J. (2004) Aberrant polycystin-1 expression results in modification of activator protein-1 activity, whereas Wnt signaling remains unaffected. *J. Biol. Chem.* **279,** 27472–27481
33. Hu, C. D., Chinenov, Y., and Kerppola, T. K. (2002) Visualization of interactions among bZIP and Rel family proteins in living cells using bimolecular fluorescence complementation. *Mol. Cell* **9,** 789–798
34. Kudo, N., Wolff, B., Sekimoto, T., Schreiner, E. P., Yoneda, Y., Yanagida, M., Horinouchi, S., and Yoshida, M. (1998) Leptomycin B inhibition of signal-mediated nuclear export by direct binding to CRM1. *Exp. Cell Res.* **242,** 540–547
35. la Cour, T., Kiemer, L., Molgaard, A., Gupta, R., Skriver, K., and Brunak, S. (2004) Analysis and prediction of leucine-rich nuclear export signals. *Protein Eng. Des. Sel.* **17,** 527–536
36. Bogerd, H. P., Fridell, R. A., Benson, R. E., Hua, J., and Cullen, B. R. (1996) Protein sequence requirements for function of the human T-cell leukemia virus type 1 Rex nuclear export signal delineated by a novel *in vivo* randomization-selection assay. *Mol. Cell Biol.* **16,** 4207–4214
37. Kazgan, N., Williams, T., Forsberg, L. J., and Brenman, J. E. (2010) Identification of a nuclear export signal in the catalytic subunit of AMP-activated protein kinase. *Mol. Biol. Cell* **21,** 3433–3442
38. Frederick, E. D., Ramos, S. B., and Blackshear, P. J. (2008) A unique C-terminal repeat domain maintains the cytosolic localization of the placenta-specific tristetraprolin family member ZFP36L3. *J. Biol. Chem.* **283,** 14792–14800
39. Murai, N., Murakami, Y., and Matsufuji, S. (2003) Identification of nuclear export signals in antizyme-1. *J. Biol. Chem.* **278,** 44791–44798
40. Poupon, V., Polo, S., Vecchi, M., Martin, G., Dautry-Varsat, A., Cerf-Bensussan, N., Di Fiore, P. P., and Benmerah, A. (2002) Differential nucleocytoplasmic trafficking between the related endocytic proteins Eps15 and Eps15R. *J. Biol. Chem.* **277,** 8941–8948
41. Devary, Y., Gottlieb, R. A., Lau, L. F., and Karin, M. (1991) Rapid and preferential activation of the c-*jun* gene during the mammalian UV response. *Mol. Cell Biol.* **11,** 2804–2811
42. Vinson, C., Myakishev, M., Acharya, A., Mir, A. A., Moll, J. R., and Bonovich, M. (2002) Classification of human B-ZIP proteins based on dimerization properties. *Mol. Cell Biol.* **22,** 6321–6335
43. Moitra, J., Szilák, L., Krylov, D., and Vinson, C. (1997) Leucine is the most stabilizing aliphatic amino acid in the d position of a dimeric leucine zipper coiled coil. *Biochemistry* **36,** 12567–12573
44. van Dam, H., Duyndam, M., Rottier, R., Bosch, A., de Vries-Smits, L., Herrlich, P., Zantema, A., Angel, P., and van der Eb, A. J. (1993) Heterodimer formation of cJun and ATF-2 is responsible for induction of c-jun by the 243-amino acid adenovirus E1A protein. *EMBO J.* **12,** 479–487
45. Raingeaud, J., Gupta, S., Rogers, J. S., Dickens, M., Han, J., Ulevitch, R. J., and Davis, R. J. (1995) Pro-inflammatory cytokines and environmental stress cause p38 mitogen-activated protein kinase activation by dual phosphorylation on tyrosine and threonine. *J. Biol. Chem.* **270,** 7420–7426
46. Xu, D., Farmer, A., and Chook, Y. M. (2010) Recognition of nuclear targeting signals by Karyopherin-$\beta$ proteins. *Curr. Opin. Struct. Biol.* **20,** 782–790
47. Shaulsky, G., Goldfinger, N., Ben-Ze'ev, A., and Rotter, V. (1990) Nuclear accumulation of p53 protein is mediated by several nuclear localization signals and plays a role in tumorigenesis. *Mol. Cell Biol.* **10,** 6565–6577
48. Liang, S. H., and Clarke, M. F. (1999) A bipartite nuclear localization signal is required for p53 nuclear import regulated by a carboxyl-terminal domain. *J. Biol. Chem.* **274,** 32699–32703
49. Stommel, J. M., Marchenko, N. D., Jimenez, G. S., Moll, U. M., Hope, T. J., and Wahl, G. M. (1999) A leucine-rich nuclear export signal in the p53 tetramerization domain. Regulation of subcellular localization and p53 activity by NES masking. *EMBO J.* **18,** 1660–1672
50. Zhang, Y., and Xiong, Y. (2001) A p53 amino-terminal nuclear export signal inhibited by DNA damage-induced phosphorylation. *Science* **292,** 1910–1915
51. Sevilla, A., Santos, C. R., Vega, F. M., and Lazo, P. A. (2004) Human vaccinia-related kinase 1 (VRK1) activates the ATF2 transcriptional activity by novel phosphorylation on Thr-73 and Ser-62 and cooperates with JNK. *J. Biol. Chem.* **279,** 27458–27465
52. Yamasaki, T., Takahashi, A., Pan, J., Yamaguchi, N., and Yokoyama, K. K. (2009) Phosphorylation of activation transcription factor-2 at serine 121 by protein kinase C controls c-Jun-mediated activation of transcription. *J. Biol. Chem.* **284,** 8567–8581
53. Okuda, A., Fukushima, A., Nishimoto, M., Orimo, A., Yamagishi, T., Nabeshima, Y., Kuro-o, M., Nabeshima, Y., Boon, K., Keaveney, M., Stunnenberg, H. G., and Muramatsu, M. (1998) UTF1, a novel transcriptional coactivator expressed in pluripotent embryonic stem cells and extraembryonic cells. *EMBO J.* **17,** 2019–2032
54. Hong, S., Choi, H. M., Park, M. J., Kim, Y. H., Choi, Y. H., Kim, H. H., Choi, Y. H., and Cheong, J. (2004) Activation and interaction of ATF2 with the coactivator ASC-2 are responsive for granulocytic differentiation by retinoic acid. *J. Biol. Chem.* **279,** 16996–17003
55. Ishida, S., Yamashita, T., Nakaya, U., and Tokino, T. (2000) Adenovirus-mediated transfer of p53-related genes induces apoptosis of human cancer cells. *Jpn. J. Cancer Res.* **91,** 174–180
56. Lee, T. I., Rinaldi, N. J., Robert, F., Odom, D. T., Bar-Joseph, Z., Gerber, G. K., Hannett, N. M., Harbison, C. T., Thompson, C. M., Simon, I., Zeitlinger, J., Jennings, E. G., Murray, H. L., Gordon, D. B., Ren, B., Wyrick, J. J., Tagne, J. B., Volkert, T. L., Fraenkel, E., Gifford, D. K., and Young, R. A. (2002) Transcriptional regulatory networks in *Saccharomyces cerevisiae*. *Science* **298,** 799–804


Downloaded from www.jbc.org at Purdue University Libraries, on September 24, 2012